Journal of Solid Mechanics Vol. 17, No. 3 (2025) pp. 301-320
DOI: 10.60664/jsm.2025.3021770

Research Paper

Thermomechanical Interaction in Photothermoelastic with Fractional Order Derivatives and Hyperbolic Two Temperature

S. Chopra [1 *], R. Kumar [2], N. Sharma [3]

[1] *Maharishi Markandeshwar, University Mullana, Ambala, Haryana, India.*
[2] *Department of Mathematics, Kurukshetra University, Kurukshetra, Haryana, India.*
[3] *Department of Mathematics, MM(DU), Mullana, Ambala, India.*

Received 28 February 2023; Received in revised form 13 April 2025; Accepted 7 January 2026

ABSTRACT

In this paper, a unified model of fractional order photothermoelastic based on hyperbolic two temperature (HTT) is developed. Fractional order derivatives, namely Riemann-Liouville (RL), Caputo-Fabrizio(CF), Atangana-Baleanu (AB) and Tempered-Caputo(TC) are used to propose this model. Two dimensional axisymmetric problem is explored in the assumed model by employing Laplace and Henkel transforms. Integral transform technique reduces the system of equations into ordinary differential equation. The arbitrary constants in the solution are determined by considering the loading environment on the surface. Three different categories of the sources are taken to explore the application of the problem as (i) normal force (ramp type) (ii) distributed thermal source (iii) concentrated carrier density source. In the new domain, the closed form expressions of physical quantities like displacement, normal stress, conductive temperature field and carrier density distribution are derived. The numerical inversion method is employed to recover the results in a physical domain. The solutions are presented graphically to know the impact of various fractional order derivatives in case of hyperbolic two- temperature(HTT), two-temperature(2T) and one-temperature (1T) for different fractional derivatives (RL,CF,AB and TC) on physical field quantities w.r.t. radial distance. Unique cases are also explored. The results provide are helpful for understanding the photothermoelastic interactions due to various sources and open up wide applications of using new fractional derivatives.

Keywords: Photothermoelastic; Hyperbolic two temperature; Riemann-Liouville; Caputo-Fabrizio; Atangana-Baleanu; Tempered-Caputo.

1 INTRODUCTION

STUDY of mechanical and thermal interaction within a solid medium is of emended significance in numerous fields of science. There are few examples such as high energy particle accelerated devices, modern aeronautical and astronomical engineering and different system utilized in nuclear and industrial utilization with the

*Corresponding author.
E-mail address: chopra.s22@gmail.com (S. Chopra)

JOURNAL OF SOLID MECHANICS JSM

consideration of second sound effect in thermoelastic model which plays a vital role in analyzing elastic body with in a variety of scientific and technological fields. The infinite thermal propagation speed is observed through conventional uncoupled theories in contradiction with physical observation. Gurtin and Williams [1,2] suggested that it is more justified to take heat conduction contribution to entropy by 1T and heat supply by another. Formulation of heat conduction for thermoelastic materials, which has a dependence on conductive temperature and thermodynamic temperature, has been presented by Chen and his co-researchers [3,4]. These 2T are separated by heat supply for time-independent situations, and hence when heat supply vanishes, both temperatures will be identical. But for time-dependent problems, 2T are in general distinct even though heat supply is zero. For many years, this theory was underestimated and remained ignored. But in present times, this theory noticed by many researchers, they further obtained advancement in two temperature theory and explained its applications primarily describing the continuity of stress function as it is discontinuous for one temperature (1T) theory. Youssef [5] formulated generalized thermoelastic model with two temperature.Youssef et al. [6] analyzed thermal stress to damaged solid sphere by using HTT generalised theory of thermoelasticity. Youssef and El-Bary [7] modified the two temperature generalized theory and furnished the HTT generalized thermoelasticity theory. Kumar et.al. [8] studied the thermoelastic interaction on HTT generalized thermoelasticity in an unbounded medium with a cylindrical cavity.

The semiconducting materials were used widely in advanced engineering, with the development of technologies. The study of wave propagation in a semiconducting medium will have important academic significance and application value. Of recent interest is the relevance of the excitation of short elastic pulses (high-frequency elastic waves) by photothermal means to several areas of applied physics including the photoacoustic microscope, thermal wave imaging, determination of thermoelastic material parameters, non-destructive evaluation of devices, monitoring of laser drilling, and laser annealing and melting phenomena in semiconductors. During the last few years,photoacoustic (PA) and photothermal (PT) science and technology have significantly evolved new methods in the investigation of semiconductors and microelectronic structures. PA and PT techniques were recently established as diagnostic methods with good delicacy to the dynamics of photoexcited carrier (Mandelis[9], Almond and Patel[10], Mandelis and Michaelian[11], Nikolic and Todorovic[12]).Several researchers [13-15] analysed the difference of thermoelastic and electronic deformations in semiconductor media by set aside the coupling between the plasma and the thermoelastic equations. Todorovic [16-18] presented two phenomena to dispense information about the properties of transport and carrier recombinations in the semiconducting medium. The changes in the propagations of thermal and plasma waves revert to the linear coupling between the thermal and the mass transport (i.e., thermodiffusion) have included. Sharma [19] investigated the boundary value problems in generalized thermodiffusive elastic medium. Sharma et.al.[20] studied the propagation of plane wave in anisotropic thermoviscoelastic medium in the context of the theory GN type-II and GN type-III. Sharma and Sharma [21] investigated the temperature inconstancy in tissues based on Penne's bio-heat transfer equation. Lotfy et.al. [22] investigated the interaction between a magnetic field and elastic materials with microstructure, whose microelements possess microtemperatures with photothermal excitation. Jahangir et.al. [23] discussed the reflection of thermoelastic waves in semiconducting medium. Zenkour [24] constructed the generalized photothermoelastic problem of beam with modified multi-phase-lag photothermoelasticity theory. Zakaria et.al. [25] used fractional calculus technique to construct a modified generalized fractional photothermeolastic model. Sharma and Kumar [26] analysed deformation due to inclined loads in dynamic mathematical model of photothermoelastic (semiconductor) medium. Sharma and Kumar [27] examined photothermoelastic deformation in dual phase lag model due to concentrated inclined load. Kumar et.al. [28] investigated deformation due to thermomechanical carrier density loading in orthotropic photothermoelastic plate. Kumar et.al.[29] studied the deformation due to thermomechanical and carrier density loading in orthotropic photothermoelastic plate under Moore-Gibson-Thompson thermoelastic model.

In recent years, fractional calculus has been used for a mathematical tool without any obvious use. Presently dynamic fractional equations have been a large part of how we model the effect of strange behaviors and memory, which are common in nature. Fractional derivative models are comprehensively used in the design of polymer models in the glass state, engines, COVID-19 and heat transfer among other applications. Various methods are being used by scholars to explore the fractional order derivative.The Riemann-Liouville fractional integral, which is simple and effective modification of Cauchy model of repeated integral in classical calculus, is mostly utilized techniques for considering a fractional order integral [30]. This technique has the ability to describe dynamic system with historical influences as (memory and anomalous behavior), which is commonly seen in most non-natural and physical system. However the traditional integral order computation lacks such possibilities because of the finite degree of freedom of the integral order parameter. Various approaches for fractional order derivative and integrals have been presented in the recent years. The non-singularity displayed at one end of the period of Riemann-

Liouville integration is believe to be a catalyst for the development of these new technologies. Caputo-Fabrizio [31] made the first attempt to present a fractional derivative operator based on the exponential function to overcome the problem of singular kernel. In fact, these fractional derivative operators do not have singular kernel. They have demonstrated that their derivative operator was suitable for the solution of some physical problems. Atangana and Alqahtani [32] applied the concept of CF fractional derivatives to the equation of groundwater pollution. They made some numerical simulations to show the stability and convergence of the analysis. However, some issues were also pointed out against the CF fractional derivative, as the kernel in integral was non-singular but was still non-local. Also in CF fractional derivatives the associated integral is not a fractional operator. To fix this shortcoming of the non-singularity and non-locality of the kernel, two fractional derivatives in Caputo and Riemann–Liouville sense are defined by Atangana and Baleanu [33,34], based on the generalized Mittag-Leffler function. The concept of AB fractional derivative to a simple nonlinear system is applied by Atangana and Koca [35] and showed the existence and uniqueness of the system solution of the fractional order. Algahtani [36] presented the AllenCahn model with both CF and AB fractional derivative to analyze the differences in real world problem. He solved the model numerically, using the Crank-Nicholson scheme and presented these numerical simulations to check the effectiveness of both the kernels. Abouelregal[37] constructed a new generalized fractional thermoelastic heat conduction model of thermoelasticity with two temperature (2TT) and two phase lags includes Riemann–Liouville, Caputo–Fabrizio, and Atangana–Baleanu fractional derivative operators. One of the significant applications of fractional calculus is the description of anomalous diffusion behavior of living particles; and the tempered fractional calculus describes the transition between normal and anomalous diffusions (or the anomalous diffusion in finite time or bounded physical space). Tempered fractional calculus can be recognized as the generalization of fractional calculus. To the best of our knowledge, the definitions of fractional integration with weak singular and exponential kernels were firstly reported in Buschman's earlier work [38]. Yu and Deng [39] developed a unified fractional thermoelastic theory, and applied to study transient responses caused by a moving heat source.

In this paper, deformation due to thermomechanical and carrier density sources in a unified fractional order photothermoelastic model based on HTT, which includes distinct fractional order derivatives (Riemann-Liouville, Caputo-Fabrizio, Atangana-Baleanu and Tempered-Caputo). Axi-symmetric problem is considered in the assumed model, which is simplified by integral transform technique (involving Laplace and Henkel transforms). In the new domain, physical field quantities (normal stress, conductive temperature field and carrier density) are examined. Numerical inversion technique is used to convert the resulting expressions in the original physical domain. The variations of stress components, conductive temperature field and carrier density are depicted graphically to demonstrate the effects of different fractional derivatives in case of HTT,2T and 1T due to normal force (ramp type), thermal source and carrier density source. Some special cases are also introduced.

2 ELEMENTARY EQUATIONS

The constitutive relation and the field equations for fractional order theory of photothermoelastic based on HTT by removing body forces, heat sources and carrier photogeneration sources are described by (Todorović, [17]; Youssef et al. [6]; Yu and Deng [39])

$$\left(\lambda+\mu\right)u_{j,ij}+\mu u_{i,jj}-\gamma_t T_{,i}-\gamma_n N_{,i}=\rho\ddot{u}_l\,, \tag{1}$$

$$K\dot{\Phi}_{,ii}+K^*\Phi_{,ii}=\left(1+\frac{\tau_q^\alpha}{\alpha!}D_m^\alpha\right)\left(\rho C_e\ddot{T}+\gamma_t.T_o\ddot{u}_{k,k}-\frac{E_g}{\tau}\dot{N}\right), \tag{2}$$

$$D_e N_{,ij}-\frac{\partial N}{\partial t}-\frac{N}{\tau}+\zeta\frac{T}{\tau}=0\,. \tag{3}$$

$$t_{ij}=\left(\lambda e_{kk}-\gamma_t T-\gamma_n N\right)\delta_{ij}+2\mu e_{ij}\,, \tag{4}$$

$$\ddot{T}=\ddot{\phi}-\beta^*\phi_{,jj}\,, \qquad \text{(i, j, k, l =1, 2, 3)} \tag{5}$$

where λ and $\mu-$ Lame's constants, $T-$ temperature distribution, T_o- reference temperature, u_i-components of displacement, $\rho-$ medium density, $K-$ thermal conductivity, K^*-material constant , $t_{ij}-$the components of stress tensor, D_e- the coefficients of carrier diffusion, $\delta_{ij}-$ Kronecker's delta , $C_e-$the specific heat, $N=n-n_o$, n_o-equilibrium carrier concentration, E_g- the semiconductor energy gap, $\alpha-$is the fractional order parameter, $(\gamma_t,\gamma_n)=(3\lambda+2\mu)(\alpha_t,d_n)$, α_t-coefficient of electronic deformation and d_n- linear thermal expansion coefficient , $\zeta=\dfrac{\partial n_o}{\partial T}-$ coupling parameter, τ_q- the thermal relaxation time, β^*- HTT parameter , $\tau-$ photogenerated carrier lifetime, $t-$ time variable. D_m^α denotes different fractional derivatives as shown in Table 1.

Table 1
Different fractional derivative of α order.

D_m^α	**Fractional derivatives**	**Symbol**	**Definition**
m=1	RL	D_{RL}^α	$=\dfrac{1}{\Gamma(\alpha)}\int_0^t(t-p)^{\alpha-1}\phi(p)dp$
m=2	CF	D_{CF}^α	$=\dfrac{1}{1-\alpha}\int_0^t\exp\left[-\dfrac{\alpha(t-p)}{1-\alpha}\right]\phi^{(1)}(p)dp$
m=3	AB	D_{AB}^α	$=\dfrac{1}{1-\alpha}\int_0^t E_\alpha\left[-\dfrac{\alpha(t-p)^\alpha}{1-\alpha}\right]\phi^{(1)}(p)dp$
m=4	TC	D_{TC}^α	$=\dfrac{e^{-\chi t}}{\Gamma(1-\alpha)}\int_0^t(t-p)^{-\alpha}\dfrac{d\left[e^{\chi p}\phi(p)\right]}{dp}dp$

3 FORMULATION OF THE PROBLEM

We consider a homogeneous, isotropic photothermoelastic half-space based on HTT in the undeformed state at uniform temperature T_o.The cylindrical polar coordinate system (r,θ,z) having an origin on the plane surface $z=0$, with the z-axis putting vertically into the medium is introduced. As the problem considered is plane axi-symmetric, the components $u_\theta=0,u_r,u_z,T,P$ and N are independent of θ .A normal force (ramp type), distributed thermal source and concentrated carrier density source is assumed to be acting at the origin of the polar coordinate system. Since we are considering axi-symmetric, two dimensional problem, so we assume the components of the displacement $(\boldsymbol{u})$, temperature (T) and carrier density (N) of the form

$$\boldsymbol{u}=\left(u_r(r,z,t),0,u_z(r,z,t)\right),\ T=T(r,z,t) \text{ and } N=N(r,z,t), \tag{6}$$

For two dimensional formulations, Eqs. (1) - (5) in accordance with consideration of Eq. (6), take the form

$$(\lambda+\mu)\frac{\partial e}{\partial r}+\mu\,\Delta u_r-\gamma_t\frac{\partial T}{\partial r}-\gamma_n\frac{\partial N}{\partial r}=\rho\frac{\partial^2 u_r}{\partial t^2}, \tag{7}$$

$$(\lambda+\mu)\frac{\partial e}{\partial z}+\mu\,\Delta u_z-\gamma_t\frac{\partial T}{\partial z}-\gamma_n\frac{\partial N}{\partial z}=\rho\frac{\partial^2 u_z}{\partial t^2}, \tag{8}$$

$$\left(K^*\Delta+K\frac{\partial}{\partial t}\Delta\right)\Phi=\left(1+\frac{\tau_q^\alpha}{\alpha!}D_m^\alpha\right)\left(\rho C_e\frac{\partial^2 T}{\partial t^2}+\gamma_t.T_o\frac{\partial^2 e}{\partial t^2}-\frac{E_g}{\tau}\frac{\partial N}{\partial t}\right), \tag{9}$$

$$D_e \Delta N - \frac{\partial N}{\partial t} - \frac{N}{\tau} + \zeta \frac{T}{\tau} = 0, \tag{10}$$

$$t_{zz} = \lambda e + 2\mu \frac{\partial u_z}{\partial z} - \gamma_t T - \gamma_n N, \tag{11}$$

$$t_{zr} = \mu \left(\frac{\partial u_z}{\partial r} + \frac{\partial u_r}{\partial z} \right), \tag{12}$$

$$\frac{\partial^2 T}{\partial t^2} = \frac{\partial^2 \Phi}{\partial t^2} - \beta^* \Delta \Phi, \tag{13}$$

where $\Delta = \frac{\partial^2}{\partial r^2} + \frac{1}{r}\frac{\partial}{\partial r} + \frac{\partial^2}{\partial z^2}$ and $e = \left(\frac{\partial u_r}{\partial r} + \frac{u_r}{r} + \frac{\partial u_z}{\partial z} \right)$. Following dimensionless parameters are taken as:

$$\begin{gathered} \left(r', z', u_r', u_z'\right) = \eta_1 C_o \left(r, z, u_r, u_z\right), \left(t_{rr}', t_{zz}', t_{zr}'\right) = \frac{1}{\lambda + 2\mu}\left(t_{rr}, t_{zz}, t_{zr}\right), \left(t', \tau', \tau_q'\right) = \eta_1 C_o^2 \left(t, \tau, \tau_q\right), \\ T' = \frac{\gamma_t T}{\rho C_o^2}, N' = \frac{N}{n_o}, \Phi' = \frac{\gamma_t \Phi}{\rho C_o^2}, \beta^{*\prime} = \frac{\beta^*}{C_o^2}. \end{gathered} \tag{14}$$

Also $\eta_1 = \frac{\rho C_e}{K}, C_o^2 = \frac{\lambda + 2\mu}{\rho}$. Eqs. (7) - (13) reduce to the following form by taking into consideration Eq. (14) and after suppressing the prime as:

$$g_1 \frac{\partial e}{\partial r} + g_2 \Delta u_r - \frac{\partial T}{\partial r} - g_3 \frac{\partial N}{\partial r} = \frac{\partial^2 u_r}{\partial t^2}, \tag{15}$$

$$g_1 \frac{\partial e}{\partial z} + g_2 \Delta u_z - \frac{\partial T}{\partial z} - g_3 \frac{\partial N}{\partial z} = \frac{\partial^2 u_z}{\partial t^2}, \tag{16}$$

$$\left(g_4 \Delta + \frac{\partial}{\partial t} \Delta \right) \Phi = \left(1 + \frac{\tau_q^\alpha}{\alpha!} D_m^\alpha \right) \left(g_5 \frac{\partial^2 T}{\partial t^2} + g_6 \frac{\partial^2 e}{\partial t^2} - \frac{g_7}{\tau} \frac{\partial N}{\partial t} \right) \tag{17}$$

$$g_8 \frac{T}{\tau} + \Delta N - g_9 \left(\frac{\partial N}{\partial t} + \frac{N}{\tau} \right) = 0, \tag{18}$$

$$t_{zz} = g_o e + 2 g_2 \frac{\partial u_z}{\partial z} - T - g_3 N, \tag{19}$$

$$t_{zr} = g_2 \left(\frac{\partial u_z}{\partial r} + \frac{\partial u_r}{\partial z} \right), \tag{20}$$

$$\frac{\partial^2 T}{\partial t^2} = \frac{\partial^2 \Phi}{\partial t^2} - \beta^* \left(\frac{\partial^2}{\partial r^2} + \frac{1}{r}\frac{\partial}{\partial r} \right) \Phi \tag{21}$$

where

$$g_1=\frac{\lambda+\mu}{\rho C_o^2}, g_2=\frac{\mu}{\rho C_o^2}{}' g_3=\frac{\gamma_n n_o}{\rho C_o^2}, g_4=\frac{K^*}{K\eta_1 C_o^2}, g_5=\frac{\rho C_e}{K\eta_1}, g_6=\frac{\gamma_t^2 T_o}{K\eta_1 C_o^2\rho}, g_7=-\frac{E_g n_o \gamma_t}{K\eta_1 C_o^2\rho}, g_8=\frac{\zeta\rho C_o^2}{\gamma_t D_e n_o \eta_1}, g_9=\frac{1}{\eta_1 D_e}, g_o=\frac{\lambda}{\lambda+2\mu} \quad (22)$$

Potential functions Ω and Ψ are taken into account for further simplifications

$$u_r=\frac{\partial\Omega}{\partial r}+\frac{\partial^2\Psi}{\partial r\partial z} \text{ and } u_z=\frac{\partial\Omega}{\partial z}-\left(\frac{\partial^2\Psi}{\partial r^2}+\frac{1}{r}\frac{\partial\Psi}{\partial r}\right). \quad (23)$$

Eqs. (15) – (20) involving Eq. (23) are reduce to

$$\left(\Delta-\frac{\partial^2}{\partial t^2}\right)\Omega-T-g_3N=0, \quad (24)$$

$$\left(\Delta-\frac{1}{g_2}\frac{\partial^2}{\partial t^2}\right)\Psi=0, \quad (25)$$

$$\left(g_4\Delta+\frac{\partial}{\partial t}\Delta\right)\Phi=\left(1+\frac{\tau_q^\alpha}{\alpha!}D_m^\alpha\right)\left(g_5\frac{\partial^2 T}{\partial t^2}+g_6\Delta\frac{\partial^2\Omega}{\partial t^2}-\frac{g_7}{\tau}\frac{\partial N}{\partial t}\right), \quad (26)$$

$$\frac{g_8}{\tau}T+\left(\Delta-g_9\left(\frac{\partial}{\partial t}+\frac{1}{\tau}\right)\right)N=0, \quad (27)$$

$$t_{zz}=g_o\Delta\Omega+2g_2\frac{\partial^2\Omega}{\partial z^2}-T-g_3N, \quad (28)$$

$$t_{zr}=g_2\left(2\frac{\partial^2\Omega}{\partial r\partial z}+\frac{\partial^2\Psi}{\partial r^2}-\frac{\partial^2\Psi}{\partial z^2}\right), \quad (29)$$

We define integral transforms (Laplace and Hankel) as:

$$\overline{f}(r,z,p)=\int_0^\infty f(r,z,p)\,e^{-pt}dt, \quad (30)$$

$$\hat{f}(\eta,z,p)=H\left[\overline{f}(r,z,p)\right]=\int_0^\infty \overline{f}(r,z,p)\,r\,J_n(\eta r)dr, \quad (31)$$

where p and are the Laplace and the Hankel transform parameters and $J_n()$ being the Bessel function of order n of the first kind. Using Eqs. (30) - (31), on Eqs. (21), (24)-(29), we obtain

$$\left(\frac{d^2}{dz^2}-\eta^2-p^2\right)\hat{\Omega}-\left[1-\delta_1^*\left(\frac{d^2}{dz^2}-\eta^2\right)\right]\hat{\Phi}-g_3\hat{N}=0, \quad (32)$$

$$g_{10}\left(\frac{d^2}{dz^2}-\eta^2\right)\hat{\Omega}+\left[g_{11}\left(\frac{d^2}{dz^2}-\eta^2\right)+g_{12}\left[1-\delta_1^*\left(\frac{d^2}{dz^2}-\eta^2\right)\right]\right]\hat{\Phi}+g_{13}\hat{N}=0, \quad (33)$$

$$g_{14}\left[1-\delta_1^*\left(\frac{d^2}{dz^2}-\eta^2\right)\right]\hat{\Phi}+\left[\frac{d^2}{dz^2}-\eta^2-g_{15}\right]\hat{N}=0, \tag{34}$$

$$\left[\frac{d^2}{dz^2}-\eta^2-\frac{p^2}{g_2}\right]\hat{\Psi}=0, \tag{35}$$

$$\hat{T}=(1-\delta_1^*\Delta)\hat{\Phi}\text{, where } \delta_1^*=\begin{cases}0 & for\ 1T\\ a^* & for\ 2T\\ \dfrac{\beta^*}{p^2} & for\ HTT\end{cases}, \tag{36}$$

where a^* is two-temperature parameter.

Also $g_{10}=p^2\tau_s g_6, g_{11}=-(g_4+p), g_{12}=p^2\tau_s g_5, g_{13}=-\dfrac{p\tau_s g_7}{\tau}, g_{14}=\dfrac{g_{10}}{\tau}, g_{15}=g_9\left(p+\dfrac{1}{\tau}\right), \tau_s=1+\dfrac{\tau_q^\alpha}{\alpha!}p_m^\alpha.$

Table 2
Laplace transform of α order fractional derivative (for $0<\alpha<1$)

p_m^α	**Definition**	**Laplace transform**
m=1 (RL)	$=\dfrac{1}{\Gamma(\alpha)}\int_0^t(t-p)^{\alpha-1}\phi(p)dp$	$=1+\dfrac{\tau_q^\alpha}{\alpha!}p^\alpha$
m=2(CF)	$=\dfrac{1}{1-\alpha}\int_0^t\exp\left[-\dfrac{\alpha(t-p)}{1-\alpha}\right]\phi^{(1)}(p)dp$	$=1+\dfrac{\tau_q^\alpha}{\alpha!}\dfrac{p}{\left[(1-\alpha)p+\alpha\right]}$
m=3(AB)	$=\dfrac{1}{1-\alpha}\int_0^t E_\alpha\left[-\dfrac{\alpha(t-p)^\alpha}{1-\alpha}\right]\phi^{(1)}(p)dp$	$=1+\dfrac{\tau_q^\alpha}{\alpha!}\dfrac{p^\alpha}{\left[(1-\alpha)p^\alpha+\alpha\right]}$
m=4(TC)	$=\dfrac{e^{-\chi t}}{\Gamma(1-\alpha)}\int_0^t(t-p)^{-\alpha}\dfrac{d\left[e^{\chi p}\phi(p)\right]}{dp}dp$	$=1+\dfrac{\tau_q^\alpha}{\alpha!}(p+\chi)^\alpha,$
	$\chi-tempered\ parmeter, \chi\geq 0$	

After some algebraic calculation of Eqs. (32) - (35) ,determine the following:

$$\left(R_1D^6+R_2D^4+R_3D^2+R_4\right)\left(\hat{\Omega},\hat{\Phi},\hat{N}\right)=0, \tag{37}$$

and

$$(D^2-m_4^2)\hat{\Psi}=0. \tag{38}$$

Eqs. (28) and (29) with aid of Eqs (30) and (31) become

$$\hat{t}_{zz}=\left[g_o\left(\frac{d^2}{dz^2}-\eta^2\right)+2g_2\frac{d^2}{dz^2}\right]\hat{\Omega}+\left(-2\eta g_2\right)\frac{d\hat{\Psi}}{dz}-\left[1-\delta_1^*\left(\frac{d^2}{dz^2}-\eta^2\right)\right]\hat{\Phi}-g_3\hat{N}, \tag{39}$$

$$\hat{t}_{zr}=-2\eta g_2\frac{d\hat{\Omega}}{dz}-\left(g_2\frac{d^2}{dz^2}+g_2\eta^2\right)\hat{\Psi}, \tag{40}$$

where

$$\begin{aligned}
&R_1 = g_{18} - \delta_1^* g_{10}\,,\\
&R_2 = g_{19} + g_{10}g_{17} - g_{13}g_{20} - g_{16}g_{18} - g_{18}g_{22} - g_3 g_{10}g_{20} + g_{10}g_{22}\delta_1^* + g_{10}\eta^2\delta_1^*,\\
&R_3 = -g_{13}g_{21} - g_{16}g_{19} - g_{19}g_{22} - g_3 g_{10}g_{21} - g_{10}g_{17}g_{22} + g_{13}g_{16}g_{20} + g_{16}g_{18}g_{22} - g_{10}g_{17}\eta^2 - g_{10}g_{22}\eta^2\delta_1^* + g_3 g_{10}g_{20}\eta^2,\\
&R_4 = g_{13}g_{26}g_{21} + g_{16}g_{19}g_{22} + \eta^2 g_3 g_{10}g_{21} + \eta^2 g_{10}g_{17}g_{22},
\end{aligned} \tag{41}$$

Also

$$g_{16} = \eta^2 + p^2, g_{17} = \delta_1^*\eta^2 + 1, g_{18} = \delta_1^* g_{12} + g_{11}, g_{19} = g_{12} - \eta^2\delta_1^* g_{12} - g_{11}\eta^2, g_{20} = -\delta_1^* g_{14}, g_{21} = g_{14} + \eta^2\delta_1^* g_{14}, g_{22} = g_{15} + \eta^2.$$

The general solution of Eqs. (37) and (38) satisfying the radiation conditions can be written as:

$$\left(\hat{\Omega}, \hat{\Phi}, \hat{N}\right) = \sum_{j=1}^{3}\left(1, h_{1j}, h_{2j}\right) C_j e^{-m_j z}, \tag{42}$$

$$\hat{\Psi} = C_4 e^{-m_4 z}, \tag{43}$$

where $m_j\,(j = 1,2,3)$ are roots of $\left(R_1 D^6 + R_2 D^4 + R_3 D^2 + R_4\right) = 0$ and coupling parameters are

$$h_{1j} = \sum_{j=1}^{3} \frac{R_8 m_j^4 + R_9 m_j^2 + R_{10}}{R_5 m_j^4 + R_6 m_j^2 + R_7} \tag{44}$$

$$h_{2j} = \sum_{j=1}^{3} \frac{R_{11} m_j^4 + R_{12} m_j^2 + R_{13}}{R_5 m_j^4 + R_6 m_j^2 + R_7} \tag{45}$$

Also

$$m_4^2 = \eta^2 + \frac{p^2}{g_2}, \tag{46}$$

where

$$\begin{aligned}
&R_5 = g_{18}, R_6 = g_{19} - g_{13}g_{20} - g_{18}g_{22}, R_7 = -g_{19}g_{22} - g_{13}g_{21}, R_8 = g_{10}, R_9 = -\eta^2 g_{10} + g_{10}g_{22}, R_{10} = \eta^2 g_{10}g_{22},\\
&R_{11} = g_{10}g_{20}, R_{12} = -\eta^2 g_{10}g_{20} + g_{21}g_{10}, R_{13} = -\eta^2 g_{21}g_{10},
\end{aligned} \tag{47}$$

Substituting the values of $\hat{\Phi}, \hat{N}, \hat{\Omega}$ and $\hat{\Psi}$ from Eqs. (42) and (43) in Eqs. (23), (39) and (40) after using Eqs. (30) and (31), yield

$$\hat{u}_r = -\eta\left(\sum_{j=1}^{3} C_j e^{-m_j z}\right) + m_4 C_4 e^{-m_4 z}, \tag{48}$$

$$\hat{u}_z = \sum_{j=1}^{3} m_j C_j e^{-m_j z} + \eta^2 C_4 e^{-m_4 z}, \tag{49}$$

$$\hat{t}_{zz} = \sum_{j=1}^{3} d_{1j} C_j e^{-m_j z} + d_{14} C_4 e^{-m_4 z}, \tag{50}$$

$$\hat{t}_{zr} = \sum_{j=1}^{3} d_{2j} C_j e^{-m_j z} + d_{24} C_4 e^{-m_4 z}, \tag{51}$$

where

$$d_{1j} = \left(g_o + 2g_2\right) m_j^2 - g_o \eta^2 - \left(1 - \delta_1^* \left(m_j^2 - \eta^2\right)\right) h_{1j} - g_3 h_{2j} \quad , d_{14} = -2\eta g_2 m_4 \, , d_{2j} = -2\eta g_2 m_j \text{ and } d_{24} = -g_2 \left(m_4^2 + \eta^2\right) (\text{for } j = 1,2,3.)$$

4 RESTRICTIONS ON THE BOUNDARY

The boundary restrictions for the assumed model are subjected to normal force (ramp type), distributed thermal source, concentrated carrier density sources at the plane $z = 0$ are considered as:

$$\left.\begin{aligned} t_{zz} &= -F_1\left(r,z,t\right) \, , \\ t_{zr} &= 0 \quad , \\ \phi &= F_2\left(r,z,t\right) \, , \\ N &= F_3\left(r,z,t\right) \, , \end{aligned}\right\} \text{ at } z = 0 \tag{52}$$

where

$$F_1\left(r,z,t\right) = F_{10} \frac{\delta(r)}{2\pi r} \begin{cases} 0 \, , & t \le 0 \\ \dfrac{t}{t_o}, & 0 < t \le t_o \, , \\ 1 \, , & t > t_o \end{cases} \tag{53}$$

$$F_2\left(r,z,t\right) = F_{20} \, H(a-r)\delta\left(t\right), \tag{54}$$

$$F_3\left(r,z,t\right) = F_{30} \frac{\delta\left(r\right)}{2\pi r} \delta\left(t\right). \tag{55}$$

Also, H ( ) is Heaviside step function , F_{10} is the magnitude of the force, F_{20} is the constant temperature applied on the boundary and F_{30} is constant.

Applying Laplace and Hankel transform defined by Eqs. (30) - (31) on Eqs. (52) - (55), we attain

$$\left.\begin{aligned} \hat{t}_{zz} &= -\hat{F}_1\left(\eta,p\right) = F_{10} \frac{(1 - e^{-pt_o})}{2\pi \, t_o p^2} \, , \\ \hat{t}_{zr} &= 0 \, , \\ \hat{\phi} &= \hat{F}_2\left(\eta,p\right) = \frac{\mathrm{F}_{20}}{\eta} a J_1(\eta a) \, , \\ \hat{N} &= \hat{F}_3\left(\eta,p\right) = \frac{F_{30}}{2\pi} \, , \end{aligned}\right\} \text{ at } z = 0 \tag{56}$$

Substituting the values of $\hat{t}_{zz}, \hat{t}_{zr}, \hat{\phi}$ and $\hat{N}$ from Eqs. (50) - (51) and (42) in the transformed boundary restrictions (56), yield

$$\sum_{j=1}^{3} d_{1j} C_j e^{-m_j z} + d_{14} C_4 e^{-m_4 z} = -\hat{F}_1(\eta, p), \tag{57}$$

$$\sum_{j=1}^{3} d_{2j} C_j e^{-m_j z} + d_{24} C_4 e^{-m_4 z} = 0 \quad , \tag{58}$$

$$\sum_{j=1}^{3} \left(h_{1j} C_j e^{-m_j z} \right) = \hat{F}_2(\eta, p) \ , \tag{59}$$

$$\sum_{j=1}^{3} \left(h_{2j} C_j e^{-m_j z} \right) = \hat{F}_3(\eta, p) \ . \tag{60}$$

Eqs. (57) - (60) are taken in matrix form as:

$$AC=B, \tag{61}$$

$$A = \begin{bmatrix} d_{11}e_1 & d_{12}e_2 & d_{13}e_3 & d_{14}e_4 \\ d_{21}e_1 & d_{22}e_2 & d_{23}e_3 & d_{24}e_4 \\ h_{11}e_1 & h_{12}e_2 & h_{13}e_3 & h_{14}e_4 \\ h_{21}e_1 & h_{22}e_2 & h_{23}e_3 & h_{24}e_4 \end{bmatrix}, C = \begin{bmatrix} C_1 \\ C_2 \\ C_3 \\ C_4 \end{bmatrix}, B = \begin{bmatrix} -F_1(x_1, t) \\ 0 \\ F_2(x_1, t) \\ F_3(x_1, t) \end{bmatrix} \tag{62}$$

and $e_j = e^{-m_j z}$ $j = 1, 2, 3, 4.$ From Eq. (62), we determine

$$C_j = \frac{\Delta_j}{\Delta}, j = 1, 2, 3, 4. \tag{63}$$

where

$$\Delta = \det A, \Delta_j = \text{ determinant of } A \text{ when } j^{th} \text{ column of } A \text{ replaced by } B \tag{64}$$

and

$$\Delta = E_o \begin{pmatrix} d_{11}d_{22}h_{13}h_{24} - d_{11}d_{22}h_{14}h_{23} - d_{11}d_{23}h_{12}h_{24} + d_{11}d_{23}h_{14}h_{22} + d_{11}d_{24}h_{12}h_{23} - d_{11}d_{24}h_{13}h_{22} - \\ d_{12}d_{21}h_{13}h_{24} + d_{12}d_{21}h_{14}h_{23} + d_{12}d_{23}h_{11}h_{24} - d_{12}d_{23}h_{14}h_{21} - d_{12}d_{24}h_{11}h_{23} + d_{12}d_{24}h_{13}h_{21} + \\ d_{13}d_{21}h_{12}h_{24} - d_{13}d_{21}h_{14}h_{22} - d_{13}d_{22}h_{11}h_{24} + d_{13}d_{22}h_{14}h_{21} + d_{13}d_{24}h_{11}h_{22} - d_{13}d_{24}h_{12}h_{21} - \\ d_{14}d_{21}h_{12}h_{23} + d_{14}d_{21}h_{13}h_{22} + d_{14}d_{22}h_{11}h_{23} - d_{14}d_{22}h_{13}h_{21} - d_{14}d_{23}h_{11}h_{22} + d_{14}d_{23}h_{12}h_{21} \end{pmatrix} \tag{65}$$

$$\Delta_1 = \left(F_1 R_{14} + F_2 R_{15} + F_3 R_{16} \right), \tag{66}$$

$$\Delta_2 = \left(F_1 R_{17} + F_2 R_{18} + F_3 R_{19} \right), \tag{67}$$

$$\Delta_3 = \left(F_1 R_{20} + F_2 R_{21} + F_3 R_{22} \right), \tag{68}$$

$$\Delta_4 = \left(F_1 R_{23} + F_2 R_{24} + F_3 R_{25} \right), \tag{69}$$

where

$$
\begin{aligned}
R_{14} &= E_1\left(d_{22}h_{13}h_{24} - d_{22}h_{14}h_{23} - d_{23}h_{12}h_{24} + d_{23}h_{14}h_{22} + d_{24}h_{12}h_{23} - d_{24}h_{13}h_{22}\right),\\
R_{15} &= E_1\left(d_{12}d_{23}h_{24} - d_{12}d_{24}h_{23} - d_{13}d_{22}h_{24} + d_{13}d_{24}h_{22} + d_{14}d_{22}h_{23} - d_{14}d_{23}h_{22}\right),\\
R_{16} &= E_1\left(d_{12}d_{24}h_{13} - d_{12}d_{23}h_{14} + d_{13}d_{22}h_{14} - d_{13}d_{24}h_{12} - d_{14}d_{22}h_{13} + d_{14}d_{23}h_{12}\right),\\
R_{17} &= E_2\left(-d_{21}h_{13}h_{24} + d_{21}h_{14}h_{23} + d_{23}h_{11}h_{24} - d_{23}h_{14}h_{21} - d_{24}h_{11}h_{23} + d_{24}h_{13}h_{21}\right),\\
R_{18} &= E_2\left(-d_{11}d_{23}h_{24} + d_{11}d_{24}h_{23} + d_{13}d_{21}h_{24} - d_{13}d_{24}h_{21} - d_{14}d_{21}h_{23} + d_{14}d_{23}h_{21}\right),\\
R_{19} &= E_2\left(d_{11}d_{23}h_{14} - d_{11}d_{24}h_{13} - d_{13}d_{21}h_{14} + d_{13}d_{24}h_{11} + d_{14}d_{21}h_{13} - d_{14}d_{23}h_{11}\right),\\
R_{20} &= E_3\left(d_{21}h_{12}h_{24} - d_{21}h_{14}h_{22} - d_{22}h_{11}h_{24} + d_{22}h_{21}h_{14} + d_{24}h_{11}h_{22} - d_{24}h_{12}h_{21}\right),\\
R_{21} &= E_3\left(d_{11}d_{22}h_{24} - d_{11}d_{24}h_{22} - d_{12}d_{21}h_{24} + d_{12}d_{24}h_{21} + d_{14}d_{21}h_{22} - d_{14}d_{22}h_{21}\right),\\
R_{22} &= E_3\left(d_{11}d_{24}h_{12} - d_{11}d_{22}h_{14} + d_{12}d_{21}h_{14} - d_{12}d_{24}h_{11} - d_{14}d_{21}h_{12} - d_{14}d_{22}h_{11}\right),\\
R_{23} &= E_4\left(-d_{21}h_{12}h_{23} + d_{21}h_{13}h_{22} + d_{22}h_{11}h_{23} - d_{22}h_{13}h_{21} - d_{23}h_{11}h_{22} + d_{23}h_{12}h_{21}\right),\\
R_{24} &= E_4\left(-d_{11}d_{22}h_{23} + d_{11}d_{23}h_{22} + d_{12}d_{21}h_{23} - d_{12}d_{23}h_{21} - d_{13}d_{21}h_{22} + d_{13}d_{22}h_{21}\right),\\
R_{25} &= E_4\left(d_{11}d_{22}h_{13} - d_{11}d_{23}h_{12} - d_{12}d_{21}h_{13} + d_{12}d_{23}h_{11} + d_{13}d_{21}h_{12} - d_{13}d_{22}h_{11}\right),
\end{aligned}
\tag{70}
$$

and $e^{-(m_1+m_2+m_3+m_4)z} = E_O, e^{-(m_2+m_3+m_4)z} = E_1, e^{-(m_1+m_3+m_4)z} = E_2, e^{-(m_1+m_2+m_4)z} = E_3, e^{-(m_1+m_2+m_3)z} = E_4$. Substituting the values of C_j from Eqs. (63) in Eqs. (48) - (51) and (42), determine the displacement components, stress components, conductive temperature and carrier density distribution as:

$$\hat{u}_r = \frac{1}{\Delta}\left(L_1\hat{F}_1(\eta,p) + L_2\hat{F}_2(\eta,p) + L_3\hat{F}_3(\eta,p)\right), \tag{71}$$

$$\hat{u}_z = \frac{1}{\Delta}\left(L_4\hat{F}_1(\eta,p) + L_5\hat{F}_2(\eta,p) + L_6\hat{F}_3(\eta,p)\right), \tag{72}$$

$$\hat{t}_{zz} = \frac{1}{\Delta}\left(L_7\hat{F}_1(\eta,p) + L_8\hat{F}_2(\eta,p) + L_9\hat{F}_3(\eta,p)\right), \tag{73}$$

$$\hat{t}_{zr} = \frac{1}{\Delta}\left(L_{10}\hat{F}_1(\eta,p) + L_{11}\hat{F}_2(\eta,p) + L_{12}\hat{F}_3(\eta,p)\right), \tag{74}$$

$$\hat{\phi} = \frac{1}{\Delta}\left(L_{13}\hat{F}_1(\eta,p) + L_{14}\hat{F}_2(\eta,p) + L_{15}\hat{F}_3(\eta,p)\right), \tag{75}$$

$$\hat{N} = \frac{1}{\Delta}\left(L_{16}\hat{F}_1(\eta,p) + L_{17}\hat{F}_2(\eta,p) + L_{18}\hat{F}_3(\eta,p)\right). \tag{76}$$

where

$$
\begin{aligned}
(L_1, L_2) &= \left(-\eta R_{14}E_1 - \eta R_{17}E_2 - \eta R_{20}E_3 + m_4 R_{23}E_4, -\eta R_{15}E_1 - \eta R_{18}E_2 - \eta R_{21}E_3 + m_4 R_{24}E_4\right)\\
(L_3, L_4) &= \left(-\eta R_{16}E_1 - \eta R_{19}E_2 - \eta R_{22}E_3 + m_4 R_{25}E_4, m_1 R_{14}E_1 + m_2 R_{17}E_2 + m_3 R_{20}E_3 + \eta^2 R_{23}E_4\right)\\
(L_5, L_6) &= \left(m_1 R_{15}E_1 + m_2 R_{18}E_2 + m_3 R_{21}E_3 + \eta^2 R_{24}E_4, m_1 R_{16}E_1 + m_2 R_{19}E_2 + m_3 R_{22}E_3 + \eta^2 R_{25}E_4\right)\\
(L_7, L_8) &= \left(d_{11}R_{14}E_1 + d_{12}R_{17}E_2 + d_{13}R_{20}E_3 + d_{14}R_{23}E_4, d_{11}R_{15}E_1 + d_{12}R_{18}E_2 + d_{13}R_{21}E_3 + d_{14}R_{24}E_4\right)\\
(L_9, L_{10}) &= \left(d_{11}R_{16}E_1 + d_{12}R_{19}E_2 + d_{13}R_{22}E_3 + d_{14}R_{25}E_4, d_{21}R_{14}E_1 + d_{22}R_{17}E_2 + d_{23}R_{20}E_3 + d_{24}R_{23}E_4\right)
\end{aligned}
\tag{77}
$$

$$\begin{aligned}
&\left(L_{11}, L_{12}\right)=\left(d_{21} R_{15} E_1+d_{22} R_{18} E_2+d_{23} R_{21} E_3+d_{24} R_{24} E_4, d_{31} R_{16} E_1+d_{32} R_{19} E_2+d_{33} R_{22} E_3+d_{34} R_{25} E_4\right)\\
&\left(L_{14}, L_{15}\right)=\left(h_{11} R_{14} E_1+h_{12} R_{17} E_2+h_{13} R_{20} E_3, h_{11} R_{15} E_1+h_{12} R_{18} E_2+h_{13} R_{21} E_3\right)\\
&\left(L_{16}, L_{17}\right)=\left(h_{11} R_{16} E_1+h_{12} R_{19} E_2+h_{13} R_{22} E_3, h_{21} R_{14} E_1+h_{22} R_{17} E_2+h_{23} R_{20} E_3\right)\\
&\left(L_{15}, L_{16}\right)=\left(h_{21} R_{15} E_1+h_{22} R_{18} E_2+h_{23} R_{21} E_3, h_{21} R_{16} E_1+h_{22} R_{19} E_2+h_{23} R_{22} E_3\right)
\end{aligned} \tag{77}$$

5 PARTICULAR CASES

(i) For normal force (ramp type) $F_{20}=F_{30}=0$ yield

$$\left(\hat{u}_r, \hat{u}_z, \hat{t}_{zz}, \hat{t}_{zr}, \hat{\phi}, \hat{N}\right)=\frac{1}{\Delta}\left(\left(L_1, L_4, L_7, L_{10}, L_{13}, L_{16}\right) \hat{F}_1(\eta, p)\right), \tag{78}$$

where $\hat{F}_1(\eta, p)$ is given by Eq. (56).

(ii) For distributed thermal source $F_{10}=F_{30}=0$ yield

$$\left(\hat{u}_r, \hat{u}_z, \hat{t}_{zz}, \hat{t}_{zr}, \hat{\phi}, \hat{N}\right)=\frac{1}{\Delta}\left(\left(L_2, L_5, L_8, L_{11}, L_{14}, L_{17}\right) \hat{F}_2(\eta, p)\right), \tag{79}$$

where $\hat{F}_2(\eta, p)$ is given by Eq. (56).

(iii) For concentrated carrier density source $F_{10}=F_{20}=0$ yield

$$\left(\hat{u}_r, \hat{u}_z, \hat{t}_{zz}, \hat{t}_{zr}, \hat{\phi}, \hat{N}\right)=\frac{1}{\Delta}\left(\left(L_3, L_6, L_9, L_{12}, L_{15}, L_{18}\right) \hat{F}_3(\eta, p)\right), \tag{80}$$

where $\hat{F}_3(\eta, p)$ is given by Eq. (56).

6 UNIQUE CASES

(a) Considering $m=1,2,3,4$ in τ_s, yield the resulting expressions for RL, CF, AB and TC model of fractional order derivatives.
(c) By taking $\delta_1^2=a^*$, corresponding expressions for different fractional order photothermoelastic with two temperature are obtained.
(d) For $\delta_1^2=0$, resulting expressions for different fractional order photothermoelastic with one temperature are determined.

7 NUMERICAL RESULTS AND DISCUSSION

For the numerical calculations, we take material constants for orthotropic Silicon (Si) material as:

$$\begin{aligned}
&\lambda=3.64\ N/m^2,\ \mu=5.46\ N/m^2, \gamma_n=-0.029715 m^3, \rho=2330\, kg/m^3, T_o=300K, T_p=2\, ps, K=150\, w/mk,\\
&E_g=1.11 eV, C_e=695\, j/kg K, \tau=5s, D_e=2.5\, m^2/s, n_o=10^{20}\, m^{-3}, n_o=10^{20}\, m^{-3}.
\end{aligned}$$

Case-I: Fig. 1.1-1.9 depict the variations of all field variables with radial distance *r* on the plane $z=1$ for the different types of fractional order derivatives with HTT.

Figs. 1.1-1.3 represent normal force (NF with HTT), Figs. 1.4-1.6 represents thermal source (TS with HTT), Figs. 1.7-1.9 represent carrier density source (CDS with HTT). In all the figures solid line correspond to Riemann-Liouville (RL), dashed line corresponds to Caputo-Fabrizio(CF), dotted line corresponds to Atangana-Baleanu (AB) and dash-dot line corresponds to Tempered-Caputo(TC) fractional order derivatives.

Fig. 1.1-1.3 depicts tendency of t_{zz}, ϕ and N vs. r in case of NF with HTT for different fractional order models. TC model enhances the immensity of t_{zz} whereas minimum value of t_{zz} attained due to CF type fractional operator for the whole range of r. Near and far off the source , the immensity of ϕ and N are enhanced due to AB model whereas TC model minimize the values.

The curves correspond to N for TC model is opposite oscillatory to all other models for finite domain of r. Fig. 1.4-1.6 shows movement of t_{zz}, ϕ and N vs. r in case of TS with HTT for different fractional order models. Near and far off the source, the magnitude of t_{zz} and ϕ intensify due to CF model, whereas t_{zz} and ϕ is less impacted due to TC model. Away from source, ϕ and N attains increasing pattern for all assumed models. The behavior and variation of ϕ and N is almost similar with distinct magnitude.

Fig. 1.7-1.9 displays movement of t_{zz}, ϕ and N vs. r in case of CDS with HTT for different fractional order models. The impact of TC, AB and CF models on the immensities of t_{zz}, ϕ and N respectively is maximum. The curves correspond to ϕ moves in similar pattern due to CF and RL models. Far off the source, all the curves correspond to N gets increasing trend for all models.

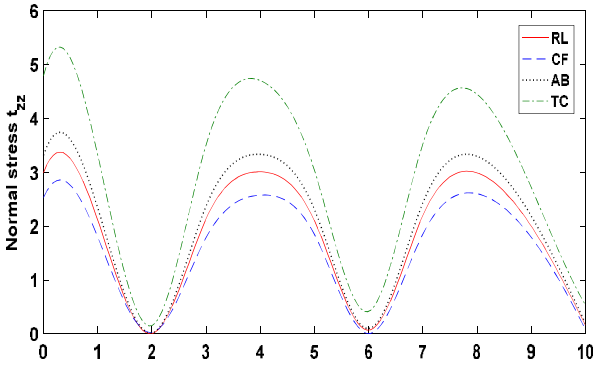

Figure 1.1 Profile of t_{zz} vs r (NF with HTT)

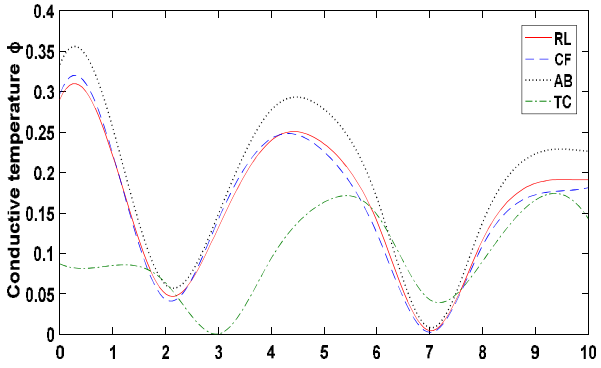

Figure 1.2 Profile of ϕ vs r (NF with HTT)

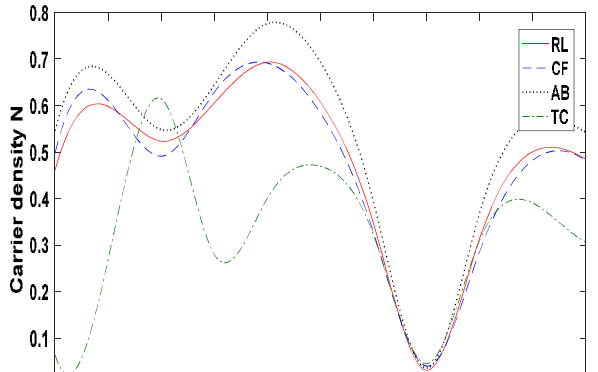

Figure 1.3 Profile of N vs r (NF with HTT)

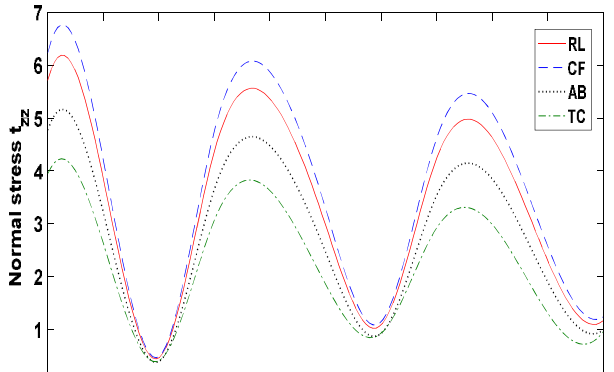

Figure 1.4 Profile of t_{zz} vs r (TS with HTT)

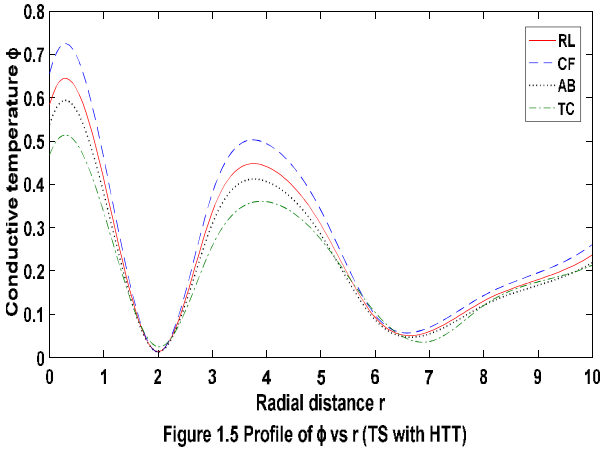

Figure 1.5 Profile of ϕ vs r (TS with HTT)

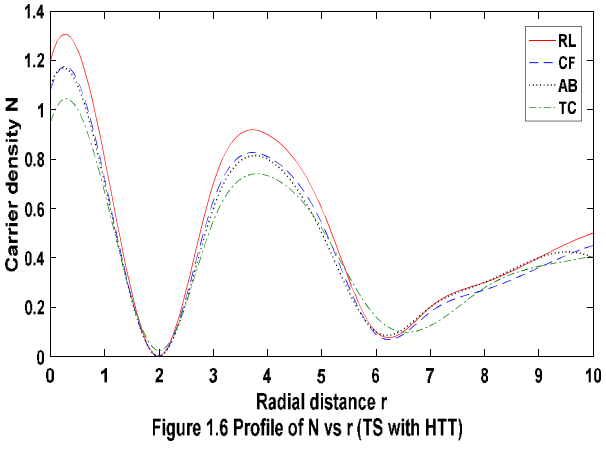

Figure 1.6 Profile of N vs r (TS with HTT)

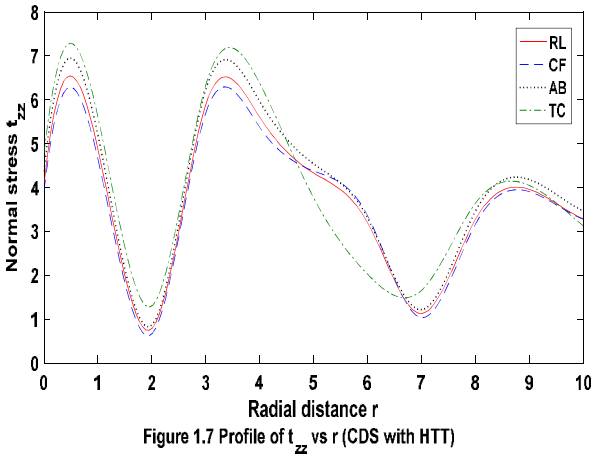

Figure 1.7 Profile of t_{zz} vs r (CDS with HTT)

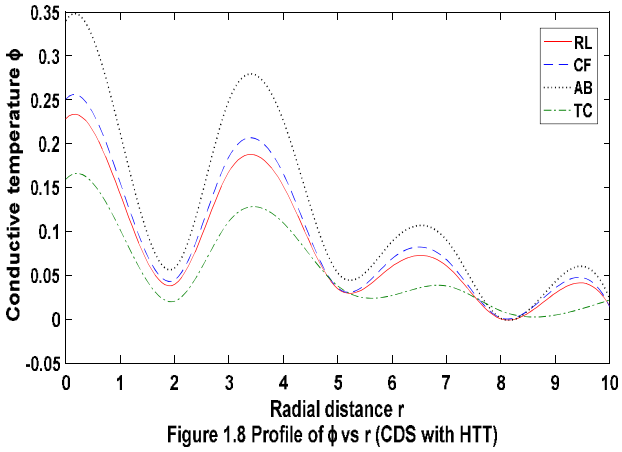

Figure 1.8 Profile of ϕ vs r (CDS with HTT)

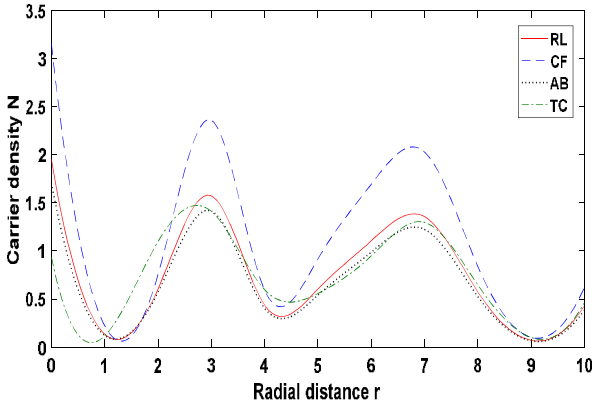

Figure 1.9 Profile of N vs r (CDS with HTT)

Case-II: Fig. 1.10-1.18 depict the variations of all field variables with radial distance r on the plane $z=1$ for the different types of fractional order derivatives with 2T.

Figs. 1.10-1.12 represent normal force (NF with 2T), Figs. 1.13-1.15 represents thermal source (TS with 2T), Figs. 1.16-1.18 represent carrier density source (CDS with 2T). In all the figures solid line correspond to Riemann-Liouville (RL), dashed line corresponds to Caputo-Fabrizio(CF), dotted line corresponds to Atangana-Baleanu (AB) and dash-dot line corresponds to Tempered-Caputo(TC) fractional order derivatives.

Fig. 1.10-1.12 depicts tendency of t_{zz}, ϕ and N vs. r in case of NF with 2T for different fractional order models. AB model enhances the immensity of t_{zz} whereas TC model have less impact on values of t_{zz}. The behavior and variation of ϕ and N are oscillatory for all type of fractional operators. The variations of N for TC model is opposite oscillatory to RL,CF and AB models for finite domain of r.

Fig. 1.13-1.15 shows movement of t_{zz}, ϕ and N vs. r in case of TS with 2T for different fractional order models. Near and far off the source, CF model raises the magnitude of t_{zz} .whereas TC minimize the values. The curve corresponds to ϕ and N gets maximum value due to TC and AB models respectively. All the curves correspond to t_{zz}, ϕ and N attain parabolic pattern for all assumed models.

Fig. 1.16-1.18 displays movement of t_{zz}, ϕ and N vs. r in case of CDS with 2T for different fractional order models. All the curves correspond to t_{zz} are monotonically decreasing in the interval $1 \le r \le 3$ and attain decreasing trend for the whole range of r. The curves relative to ϕ for CF model is opposite oscillatory to AB and RL models. The immensity of N is enhanced due to AB model and gets minimum value for CF model for the intermediate values of r.

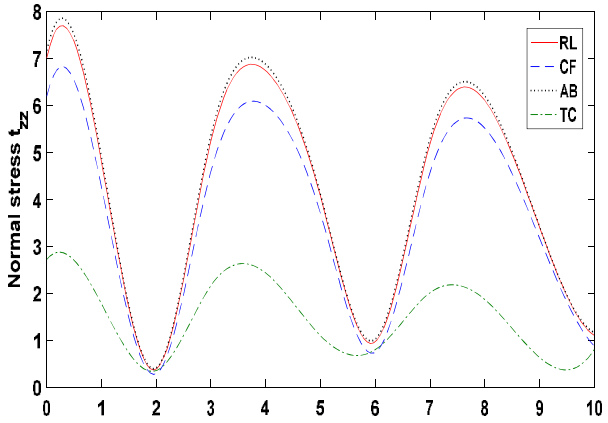

Figure 1.10 Profile of t_{zz} vs r (NF with 2T)

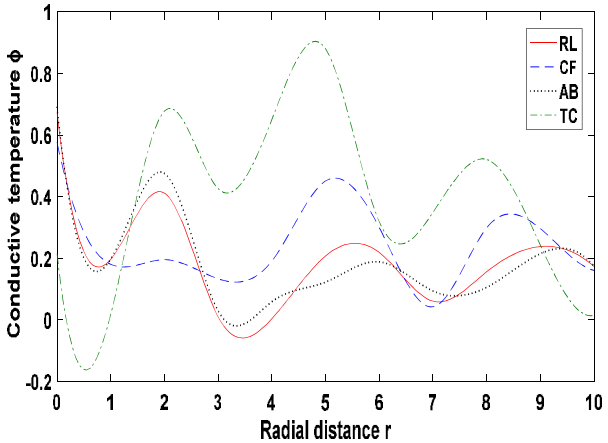

Figure 1.11 Profile of ϕ vs r (NF with HTT)

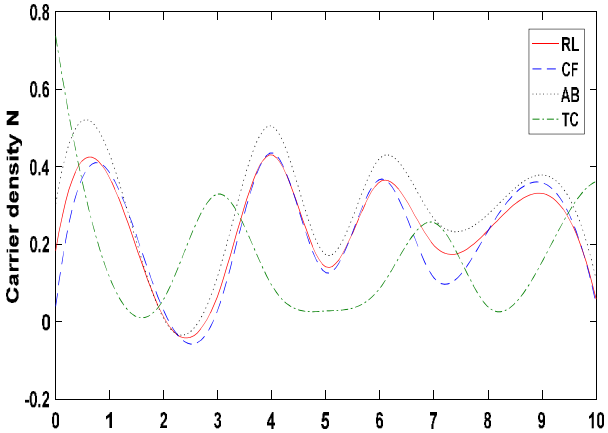

Figure 1.12 Profile of N vs r (NF with HTT)

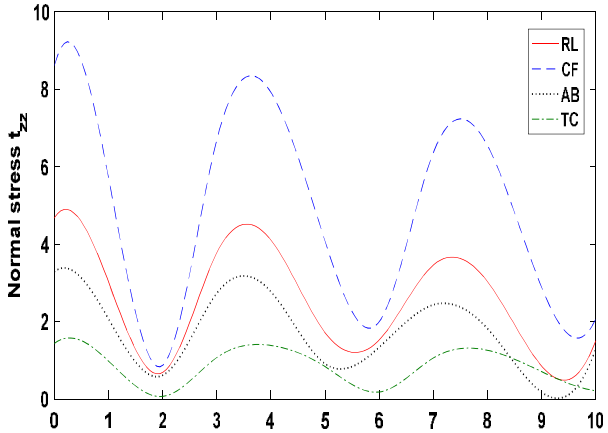

Figure 1.13 Profile of t_{zz} vs r (TS with HTT)

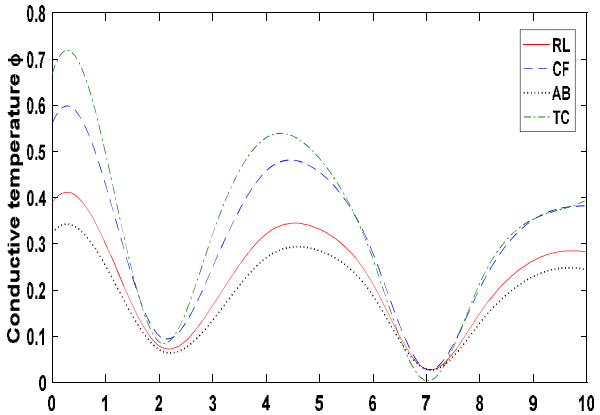

Figure 1.14 Profile of ϕ vs r (TS with 2T)

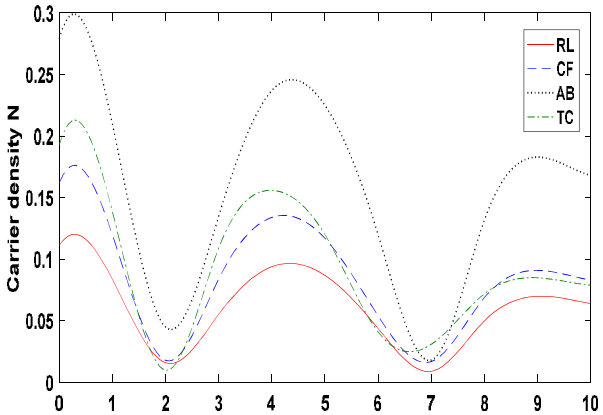

Figure 1.15 Profile of N vs r (TS with 2T)

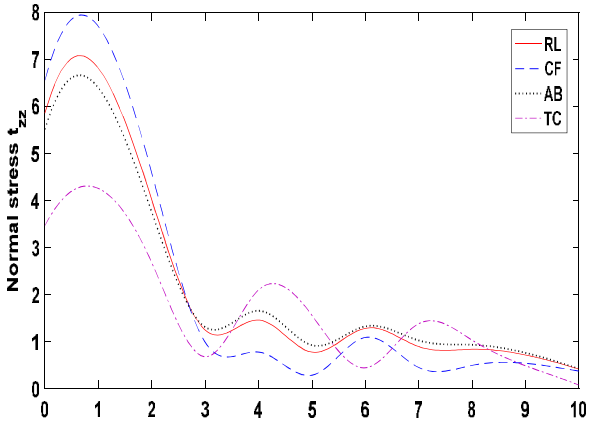

Figure 1.16 Profile of t_{zz} vs r (CDS with 2T)

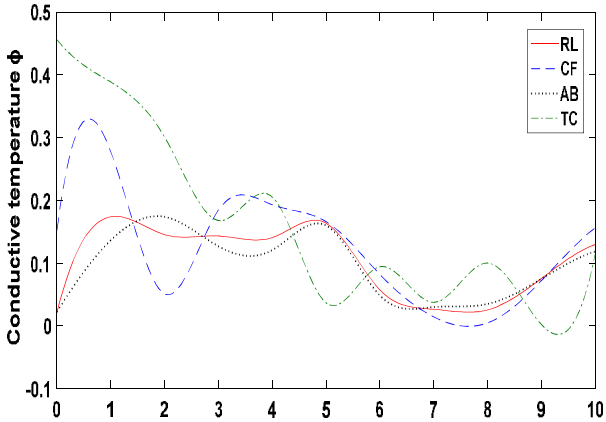

Figure 1.17 Profile of ϕ vs r (CDS with 2T)

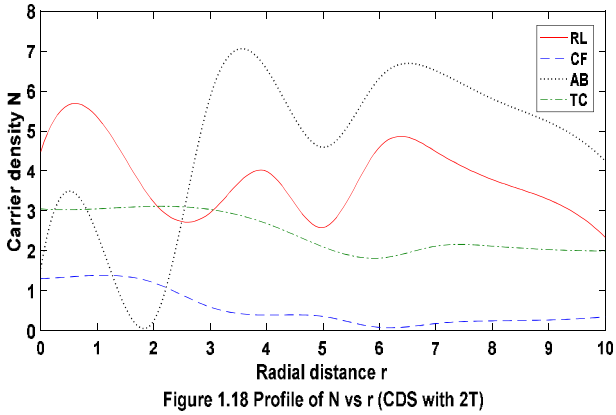

Figure 1.18 Profile of N vs r (CDS with 2T)

Case-III: Fig. 1.19-1.27 depict the variations of all field variables with radial distance r on the plane $z=1$ for the different types of fractional order derivatives with 1T.

Figs. 1.19-1.21 represent normal force (NF with 1T), Figs. 1.22-1.24 represents thermal source (TS with 1T), Figs. 1.25-1.27 represent carrier density source (CDS with 1T). In all the figures solid line correspond to Riemann-Liouville (RL), dashed line corresponds to Caputo-Fabrizio(CF), dotted line corresponds to Atangana-Baleanu (AB) and dash-dot line corresponds to Tempered-Caputo(TC) fractional order derivatives.

Fig. 1.19-1.21 depicts tendency of t_{zz}, ϕ and N vs. r in case of NF with 1T for different fractional order models. RL model intensify the immensity of t_{33} for the whole range of r, whereas TC model have less impact as compare to other models. The curves correspond to ϕ are monotonically decreasing in initial range of r due to RL and TC model. The curves relative to N are monotonically decreasing in initial range of r due to RL, CF and TC models.

Fig. 1.22-1.24 shows movement of t_{zz}, ϕ and N vs. r in case of TS with 1T for different fractional order models. Near the source, RL model intensify the magnitude of t_{zz} .whereas TC model minimize the value of t_{zz} for the whole range of r. The curve corresponds to ϕ due to AB model is opposite oscillatory to RL model in the finite domain of r. Similarly, curves correspond to N for TC model is opposite oscillatory due to AB and CF models.

Fig. 1.25-1.27 displays movement of t_{zz}, ϕ and N vs. r in case of CDS with 1T for different fractional order models. The behavior and variation of t_{zz} for AB model is opposite to RL,CF and TC model in the initial range of r. ϕ attain its maximum magnitude due to TC model and impacted less due to CF and AB models for the whole range of r. The curves correspond to N for TC model is opposite oscillatory to CF model.

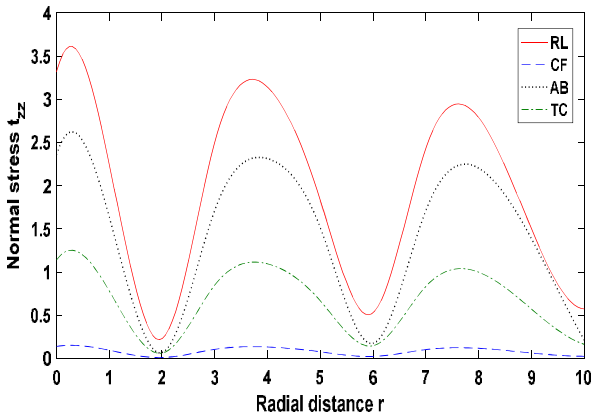

Figure 1.19 Profile of t_{zz} vs r (NF with 1T)

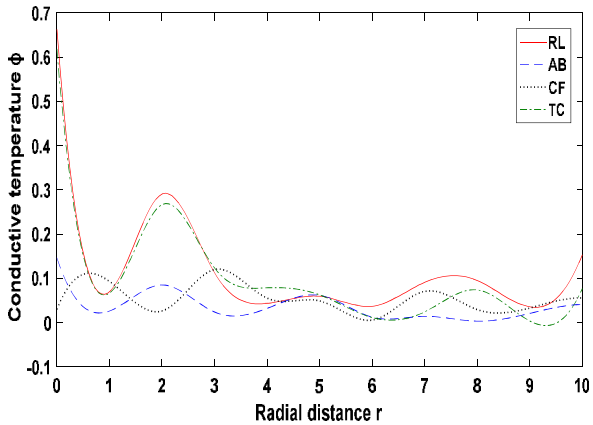

Figure 1.20 Profile of ϕ vs r (NF with 1T)

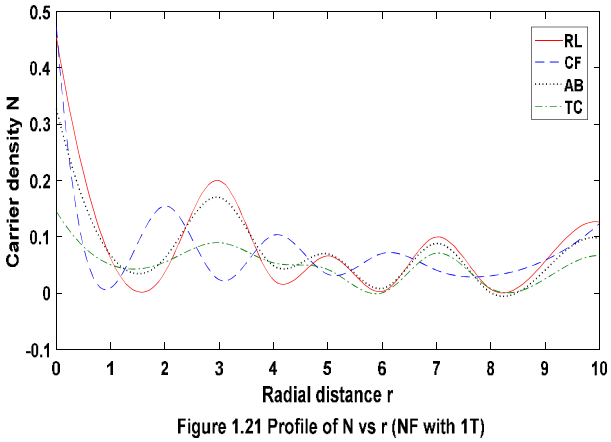

Figure 1.21 Profile of N vs r (NF with 1T)

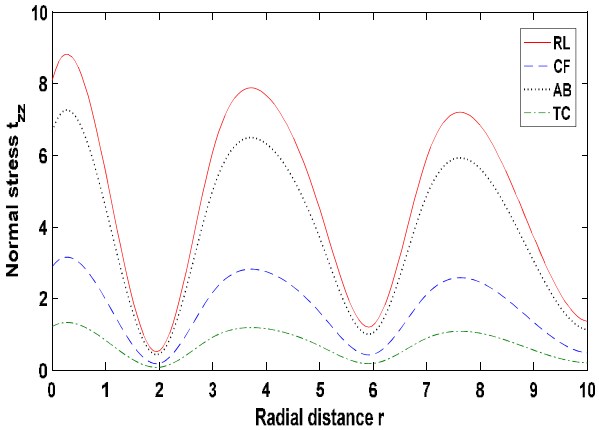

Figure 1.22 Profile of t_{zz} vs r (TS with 1T)

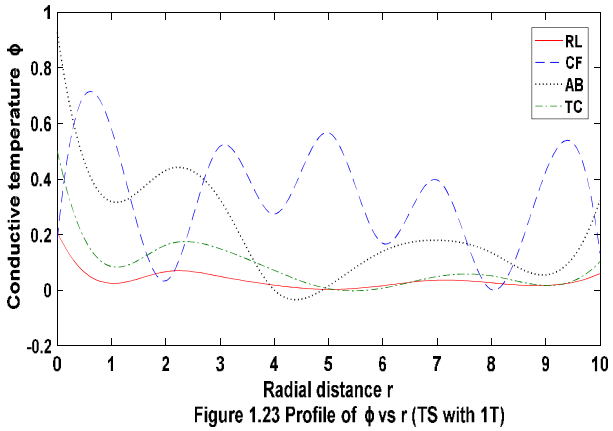

Figure 1.23 Profile of ϕ vs r (TS with 1T)

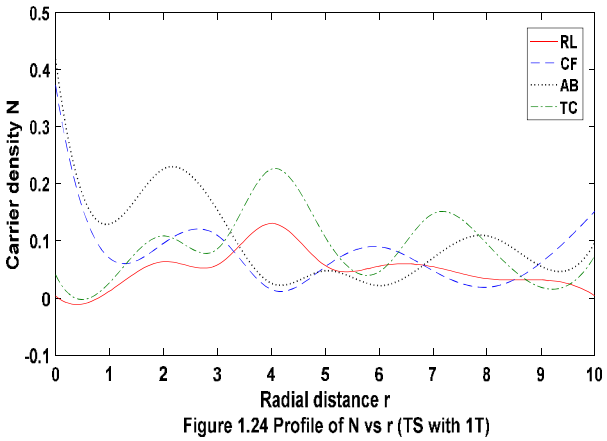

Figure 1.24 Profile of N vs r (TS with 1T)

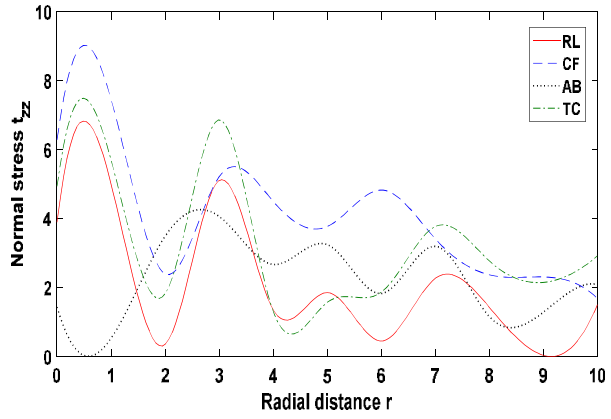

Figure 1.25 Profile of t_{zz} vs r (CDS with 1T)

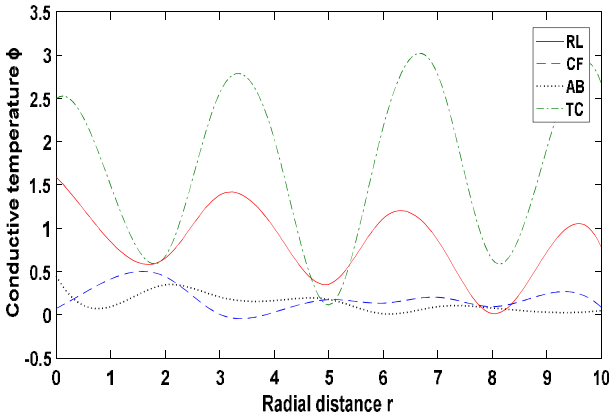

Figure 1.26 Profile of ϕ vs r (CDS with 1T)

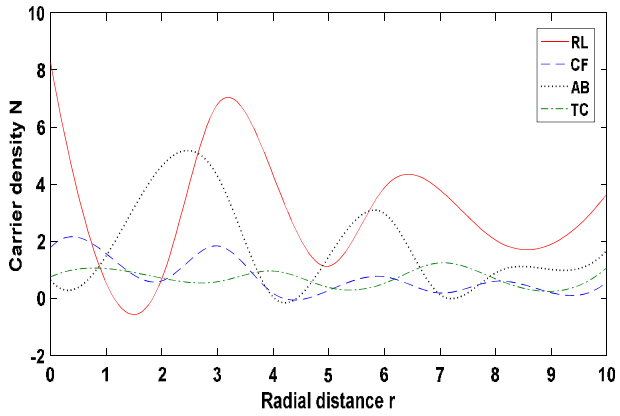

Figure 1.27 Profile of N vs r (CDS with 1T)

8 CONCLUSIONS

In this paper, fractional order derivatives Riemann-Liouville (RL), Caputo-Fabrizio(CF),Atangana-Baleanu (AB) and Tempered-Caputo(TC) have been incorporated in a uniform manner in the photothermoelastic with hyperbolic two temperature model. Laplace and Henkel transforms are used to solve the problem. Normal force, thermal source, carrier density sources are taken to study the impact of HTT, 2T and 1T under different fractional order derivatives. From numerically computed results we conclude following:

In case of HTT, the immensity of t_{zz} enhances due to TC model, whereas this model have less impact on ϕ and N as compare to other assumed models for NF. The curves correspond to t_{zz} and ϕ are more impacted due to CF model , however N attain maximum magnitude due to RL model for TS. The Impact of CF model is minimum on t_{zz} and ϕ and maximum on N in case of CDS.

For 2T, the fractional order derivative CF have more impact on t_{zz} and N and less impact on ϕ for NF. The curves correspond to t_{zz}, ϕ and N appear with parabolic pattern due to all models for TS. For CDS, the curves correspond to t_{zz} decreases monotonically in the initial range of radial distance. A non-uniform pattern is noticed due to all assumed models for ϕ and N.

For 1T, The impact of TC model is more on t_{zz} as compare to ϕ and N for NF. In case of TS, magnitude of t_{zz}, ϕ and N increases due to CF and RL models respectively. For CDS, non-uniform pattern is noticed for all models.

It is observed that present study is significant to the physical understanding of transient photothermoelastic interaction with distinct fractional order derivatives.

REFERENCES

[1] M.E. Gurtin, W.O. Williams, On the Clausius-Duhemel inequality, Z. Angrew. Math.Mech. ZAMP,17(5),626-633 (1966).
[2] M.E. Gurtin, W.O. Williams, An axiomatic foundation for continuum thermodynamics, Archive for Rational Mechanics and Analysis, 26, 83-117 (1967).
[3] P.J. Chen, M. E. Gurtin, On a theory of heat conduction involving two-temperatures, Zeitschrift fur Angew. Math.und Phys. ZAMP, 19, 614-627 (1968).
[4] P.J.Chen, M.E. Gurtin, W.O.Williams, On the thermodynamics of non-simple elastic materials with two temperatures, Zeitschrift fur Angew. Math. and Phys. ZAMP, 20,107-112 (1969).
[5] H.M. Youssef, Theory of two-temperature-generalised thermoelasticity, IMA Journal of Applied Mathematics,71(3),383-390 (2006).
[6] H.M.Youssef, A.A. El-Bary, E.A. N. AL-Lehaibi, Thermal-stress analysis of a damaged solid sphere using hyperbolic two-temperature generalised thermoelasticity theory, Scientific Reports, 11, 2289 (2021).
[7] H.M. Youssef, A.A. El-Bary, Theory of hyperbolic two-temperature generalised thermoelasticity, Mat. Phy. Mech, 40,158-171 (2018).
[8] R. Kumar, R. Prasad, R. Kumar, Thermoelastic interactions on hyperbolic two-temperature generalized thermoelasticity in an infinite medium with a cylindrical cavity, European Journal of Mechanics/ A Solids, 82, 104007 (2020).
[9] A. Mandelis, Photoacoustic and Thermal Wave Phenomena in Semiconductors, Elsevier Science, North- Holland, New York, (1987).
[10] D.P. Almond, P.M. Patel, Photothermal Science and Techniques, Chapman and Hall, London, (1996).
[11] A. Mandelis, K.H. Michaelian, Photoacoustic and photothermal science and engineering, Optical Engineering,36(2), 301-302 (1997).
[12] P.M. Nikolic, D.M. Todorovic, Photoacoustic and electroacoustic properties of semiconductors, Prog Quantum Electron, 13,107-189 (1989).
[13] F.A. McDonald, G.C. Wetsel, Generalized theory of the photoacoustic effect, J.Appl. Phys, 49(4),2313–2322 (1978).
[14] W.Jackson, N.M. Amer, Piezoelectric photoacoustic detection: theory and experiment, J.Appl. Phys, 51(6),3343–3353 (1980).
[15] R. Stearns, G. Kino, Effect of electronic strain on photoacoustic generation in silicon, Appl.Phys. Lett, 47(10),1048–1050 (1985).
[16] D. Todorović, Photothermal and electronic elastic effects in microelectromechanical structures, Rev. Sci. Instruments, 74(1), 578–581 (2003a).
[17] D. Todorović, Plasma, thermal, and elastic waves in semiconductors, Rev. Sci. Instruments, 74(1), 582–585 (2003b).
[18]D. Todorović, Plasmaelastic and thermoelastic waves in semiconductors, J. Phys. IV (Proc.) EDP Sci, 125,551–555 (2005).
[19] K. Sharma, Boundary value problems in generalised thermodiffusive elastic medium, J. Solid Mech, 2(4), 348-362 (2010).
[20] S.Sharma, K.Sharma, R.R.Bhargava, Effect of viscosity on wave propagation in anisotropic thermoelastic with Green-Naghdi theory type-II and type- III, Materials Physics and Mechanics, (16), 144-158 (2013).
[21] S.Sharma, K.Sharma, Influence of heat sources and relaxation time on temperature distribution in tissues, International Journal of Applied Mechanics and Engineering, 19(10),2478 (2014).
[22] Kh. Lotfy, R. Kumar, W. Hassan, M. Gabr, Thermomagnetic effect with microtemperature in a semiconducting photothermal excitation medium, Appl. Math Mech.- Engl. Ed, 39, 783–796 (2018).
[23] A. Jahangir, F. Tanvir, A.M. Zenkour, Reflection of photothermoelastic waves in a semiconductor material with different relaxations, Indian Journal of Physics, 95,51-59 (2020).

[24] A.M. Zenkour, Exact coupled solution for photothermal semiconducting beams using a refined multi- phase-lag theory, Optics and Laser Technology, 128, 106233 (2020).
[25] K. Zakaria, M.A. Sirwah, A.E. Abouelregal, Photo-thermoelastic model with time-fractional of higher order and phase lags for a semiconductor rotating materials, Silicon, 13, 573–585(2021).
[26] N. Sharma, R. Kumar, Photo-thermoelastic investigation of semiconductor material due to distributed loads, Journal of Solid Mechanics, 13(2), 202-212 (2021).
[27] N. Sharma, R. Kumar, Photothermoelastic deformation in dual phase lag model due to concentrated inclined load, Italian Journal of pure and Applied Mathematics, (2022).
[28] R. Kumar, N. Sharma, S. Chopra, Modelling of thermomechanical response in anisotropic photothermoelastic plate, International Journal of Mechanical Engineering, 6, (2022).
[29] R. Kumar, N. Sharma, S. Chopra, Photothermoelastic interactions under Moore-Gibson-Thompson thermoelasticity, Coupled System Mechanics ,11(5),459-483(2022).
[30] A.Khan, K.Ali Abro, A.Tassaddiq I.Khan, Atangana-baleanu and caputo fabrizio analysis of fractional derivatives for heat and mass transfer of second grade fluids over a vertical plate: a comparative study, Entropy, 19(8), 279 (2017).
[31] M.Caputo, M. Fabrizio, A new definition of fractional derivative without singular kernel, Progr. Fract. Differ. Appl, 1(2), 1–13 (2015).
[32] A.Atangana, R.T.Alqahtani, Numerical approximation of the space-time Caputo-Fabrizio fractional derivative and application to groundwater pollution equation, Advances in Difference Equations, (1), 156 (2016).
[33] A.Atangana, D.Baleanu, New fractional derivatives with nonlocal and non- singular kernel: theory and application to heat transfer model, arXiv preprint arXiv:1602.03408, (2016a).
[34] A.Atangana, D.Baleanu, Caputo-Fabrizio derivative applied to groundwater flow within confined aquifer, Journal of Engineering Mechanics, D4016005 (2016b).
[35] A.Atangana, I. Koca, Chaos in a simple nonlinear system with Atangana– Baleanu derivatives with fractional Order, Chaos, Solitons and Fractals, 1-8 (2016).
[36] O.J.J. Algahtani, Comparing the Atangana–Baleanu and Caputo–Fabrizio derivative with fractional order: Allen Cahn model, Chaos, Solitons & Fractals, 89,552- 559 (2016).
[37] A.E.Abouelregal, A comparative study of a thermoelastic problem for an infinite rigid cylinder with thermal properties using a new heat conduction model including fractional operators without non-singular kernels, Arch Appl Mech, 92, 3141–3161 (2022).
[38] R.G. Buschman, Decomposition of an integral operator by use of Mikusinski calculus, SIAM J. Math. Anal, 3, 83–85 (1972).
[39] A. Yu, June Deng, Z. Ch, Fractional order theory of Cattaneo-Type thermoelasticity using new fractional derivatives, Applied Mathematical Modelling, (87),731-751(2020).